

Feasibility of EPT in the Human Pelvis at 3T

E. Balidemaj¹, A. L. van Lier², A.J. Nederveen³, J. Crezee¹, C.A.T. van den Berg²

¹Radiotherapy, Academic Medical Center, Amsterdam, Netherlands; ²Radiotherapy, UMC Utrecht, Utrecht, Netherlands; ³Radiology, Academic Medical Center, Amsterdam, Netherlands

Introduction & Theory: Hyperthermia treatment (HT), is aimed at tumour heating to approximately 43°C using RF antenna's for energy deposition. To plan HT optimally, the electric fields need to be simulated using a patient-specific dielectric model[1]. Here, the conductivity values of the tumour are also important as they differ from normal tissue conductivity[2]. The same approach can be used to determine the SAR deposition[3]. To map the dielectric properties in tissue, "Electric Properties Tomography" (EPT)[3] was introduced. This method requires the B_1^+ amplitude and B_1^+ phase (ϕ^+) for reconstruction of dielectric property maps. For phase measurements, the phase assumption $2\phi^+ = \phi_m$ (ϕ_m : measurable transceive phase) is generally used [3,4] and was shown to hold *in vivo* for human brain at 1.5T and 3T [5]. At 7T small deviations in the reconstruction of the dielectric properties were observed which were caused by this approximation. In this study, the applicability of the phase assumption at 3T in the pelvis is investigated. Due to the larger dimensions of the pelvis, as compared to the head, the phase error should be reinvestigated for this particular anatomy.

Materials & Methods: The validity of the assumption $2\phi^+ = \phi_m$, for the human pelvis was determined using simulations and phantom measurements. For all measurements a pelvis-sized phantom was used, consisting of an elliptical cylinder ($d_{\text{major}} = 34$ cm, $d_{\text{minor}} = 25$ cm, length= 40 cm), with a sphere ($d = 10$ cm) placed on-axis (Fig. 1). The elliptical cylinder and the sphere contained Ethylene glycol (64g/L NaCl) with dielectric properties that matched the volumetric average of the pelvis at 128 MHz ($\sigma = 0.44$ S/m and $\epsilon_r = 30$, [6]). The dielectric properties were verified with an impedance probe (85070E, Agilent Technologies, Santa Clara, CA, USA). Phantom experiments were conducted on a 3.0T scanner (Philips Healthcare, Best, The Netherlands) using a Torso XL coil for reception. The B_1^+ amplitude map was acquired using the AFI method [7] (3D, nom. flip angle = 65° TR1 = 50 ms, TR2 = 290 ms, CLEAR, 2x2x5mm, 12 slices). The transceive phase was acquired by a SE experiment (2x2x5mm, CLEAR, TR = 1200 ms) [8,9]. The total measurement time was approx. 17 minutes. Conductivity values were reconstructed using the complex B_1^+ , see Eq. (2) [3], or by using the transceive phase only, Eq. (3) [4]. Numerical simulations (FDTD) were performed on a phantom, with the same dimensions and dielectric properties as used in the measurements, and on the pelvis of a adult male model (Duke, ITIS Foundation, Zurich, Switzerland)[10] by positioning it within a RF body coil model tuned for operation at 128 MHz.

Results & Discussion: In Fig. 2 we present the reconstructed σ -maps based on complex B_1^+ field (top row) and phase information only (bottom row) for both phantom simulations (left column) and phantom measurements (right column). The σ -maps of Fig.2a and Fig.2c show comparable patterns, however, a noticeable disagreement is observed on the edges of the FOV implying the phase assumption does not hold in the complete FOV. Yet, conductivity reconstruction based on phase only is shown to correlate well with actual σ -values for the central part of FOV. The σ -maps based on measurements (Fig. 2. right column) show very similar results with respect to the maps based on simulations. We notice in Fig. 2d an overestimation (see arrows) and an underestimation at the edges of the FOV, similar is observed in Fig. 2c. The ringing pattern seen on the elliptical cylinder (right column) might be due to Gibbs-ringing, however further analysis needs to provide more insight on this effect. Table 1 summarizes the conductivity values (mean \pm standard deviation), confirming an overall good agreement to the actual fluid conductivity at the isocenter of the body coil. A deviation of 5% was found for the mean conductivity of the sphere with respect to impedance probe measurement. Figure 3a shows the actual electric tissue conductivity of the pelvic model. In figure 3b-d we show the σ -map based on the simulations of the: actual B_1^+ in 3b), B_1^+ amplitude and transceive phase in 3c), and transceive phase only in 3d). We notice a good resemblance between 3c and 3b indicating the phase assumption holds very well *in vivo*. Figure 3e) indeed confirms this by showing small differences between ϕ^+ and $\phi_m/2$. In Fig. 3d, we further observe similar underestimation on the edges (white arrows) as seen in Fig. 2c.

The overall perception based on 3c-d and 3a, is that reconstructed σ -maps of large homogenous parts, coincide well with actual tissue conductivity. As EPT is based on local B_1^+ variations, reconstruction of σ -maps of smaller organs and at boundaries (red arrows in 3b-d) suffer from finite spatial kernel which includes spatial information of one tissue into its adjacent tissue and violates the assumption of piecewise dielectric properties used to derive Eq. (1). Reconstruction with edge-preserving algorithms should lead to better σ -maps of those regions.

Conclusions: We have shown that the phase assumption holds for the human pelvis and the pelvis-sized phantom at 3T using simulations and measurements. Reconstruction based on transceive phase only seems sufficient for σ -mapping of pelvic tumours, however the inclusion of B_1^+ amplitude information is necessary when reconstructing σ -maps of the whole pelvis.

References: [1] De Greef, et al., Phys Med Biol 56(11):3233-3250 (2011). [2] Joines, et. al., Med Phys. 1994; 21: 547-50. [3] Katscher et al., IEEE Trans Med Imag 28:1365-75, 2009. [4] Van Lier, MRM 2011. [5] Van Lier et al., Proc. ISMRM p.4464, 2011. [6] Gabriel, et.al.,Phys. Med. Biol. 41 (1996), 2251-2269. [7] Yamykh, MRM 57:192-200, 2007. [8] Voigt et al., Proc. ISMRM, p. 2865, 2010. [9] Van Lier et al., Proc. ISMRM p.125, 2011. [10] A. Christ et al., PMB. vol. 55 pp. N23 - N38, 2010

$$\frac{\nabla^2 B_1^+}{B_1^+} = -k^2 \quad (1)$$

$$\text{where } k^2 = \mu_0 \omega^2 + i\mu_0 \sigma \omega$$

$$-\text{Im} \left(\frac{\nabla^2 B_1^+}{B_1^+} \right) \frac{1}{\mu_0 \omega} = \sigma \quad (2)$$

$$-\text{Im} \left(\frac{\nabla^2 e^{i\phi^+}}{e^{i\phi^+}} \right) \frac{1}{\mu_0 \omega} \approx \sigma \quad (3)$$



Figure 1. Pelvis-sized phantom.

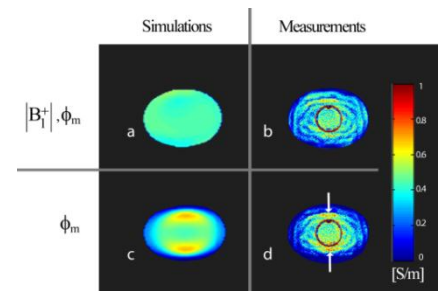


Figure 2. Conductivity maps based on simulations (left) and measurements (right).

Table 1 Reconstructed conductivity values (mean \pm standard deviation) in S/m based on measurements and simulations. Impedance probe measurement: $\sigma = 0.44$ S/m.

	Measurements	Simulations
Elliptical cylinder ($ B_1^+ , \phi_m$)	0.34 ± 0.11	0.44 ± 0.04
Sphere ($ B_1^+ , \phi_m$)	0.41 ± 0.09	0.44 ± 0.01
Elliptical cylinder (ϕ_m)	0.30 ± 0.16	0.39 ± 0.16
Sphere (ϕ_m)	0.42 ± 0.09	0.48 ± 0.04

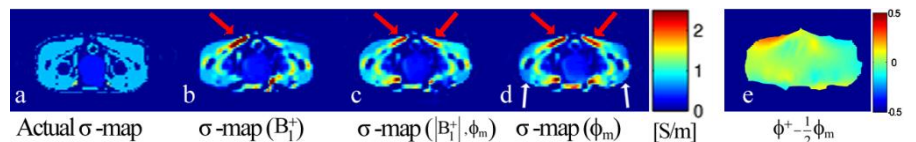


Figure 3.a)-d) Conductivity maps based on simulations with pelvic model and the difference $\phi^+ - \phi_m/2$ e).